

1 **Characteristics, main sources, health risks of PM_{2.5}-bound**
2 **perfluoroalkyl acids in Zhengzhou, central China: From**
3 **seasonal variation perspective**

4 **Jingshen Zhang^{1,3}, Xibin Ma², Minzhen Li², Zichen Wang², Nan Jiang^{2,1},**
5 **Fengchang Wu^{3,4}**

6 ¹College of Chemistry, Zhengzhou University, Zhengzhou 450001, China

7 ²College of Ecology and Environment, Zhengzhou University, Zhengzhou
8 450001, China

9 ³Huang Huai Laboratory, Henan Academy of Sciences, Zhengzhou 450046,
10 China

11 ⁴State Key Laboratory of Environmental Criteria and Risk Assessment, Chinese
12 Research Academy of Environmental Sciences, Beijing 100012, China

13 *Correspondence to:* Nan Jiang (jiangn@zzu.edu.cn), Xibin Ma
14 (maxibin163@163.com)

15

16 **1. Experiment**

17 1.1 Samples Analysis

18 1.1.1 Samples Pretreatment

19 1): Quartz filters were cut into small pieces and placed into 50 mL
20 polypropylene (PP) centrifuge tubes. An internal standard mixture solution of 50
21 μL at $0.2 \mu\text{g/mL}$ was added to the cut filters.

22 2): Organic solvents (methanol, HPLC grade) were added to extract
23 perfluoroalkyl acids from the samples via ultrasonic extraction. The ultrasonic
24 extraction process was conducted in three stages. Initially, 4 mL of methanol was
25 added and the samples were sonicated for 20 minutes; subsequently, 3 mL of
26 methanol was added for another 20 minutes of sonication; finally, an additional 3
27 mL of methanol was added for a 10-minute extraction. The extracts from each
28 sonication were collected separately.

29 3): The extracts were diluted with ultrapure water to a total volume of 250 mL
30 and then centrifuged (4500 r/min for 15 minutes) to obtain the clear supernatant.

31 4): The clear supernatant was enriched using a solid-phase extraction (SPE)
32 instrument with a wax SPE column (6 mL, 150 mg). The first step involved
33 conditioning the column with 4 mL of 0.1% aqueous ammonia-methanol solution,
34 followed by 4 mL of methanol and 4 mL of ultrapure water; the second step was
35 loading the 250 mL supernatant onto the wax SPE column at a flow rate of 1-2
36 drops per second; the third step involved washing with 4 mL of 25 mM ammonium
37 acetate solution (pH=4); the fourth step was drying under vacuum for 30 minutes
38 using the SPE instrument; the fifth step was elution with 4 mL of methanol
39 followed by 4 mL of 0.1% aqueous ammonia-methanol solution, and the eluate was
40 collected in a 10 mL PP centrifuge tube to obtain 8 mL of the final eluate.

41 5): Nitrogen Evaporationoff was performed using a nitrogen evaporator to
42 completely dry the eluate (the nitrogen blow temperature should not exceed 40°C,
43 and no bubbles should be present on the liquid surface).

44 6): The dried eluate was reconstituted with 1 mL of methanol.

45 7): The reconstituted 1 mL solution was filtered through a 0.22 µm nylon
46 syringe filter into a 2 mL brown sample vial for subsequent chromatographic
47 analysis.

48 1.1.2 Mass spectrometer condition

49 Chromatographic Column Selection: A C18 reverse-phase column (150 mm ×
50 2.1 mm, 1.8 µm) was used. Chromatographic Conditions: Mobile phase A (2 mM
51 ammonium acetate aqueous solution); Mobile phase B (acetonitrile); runtime of 20
52 minutes; flow rate of 0.3 mL/min; column temperature of 40°C; injection volume of
53 10 µL; gradient elution program (0–14 min 80% A, 14–16 min 10% A, 16–20 min
54 80% A).

55 Mass Spectrometry Conditions: Electrospray ionization (ESI) source in
56 negative ion mode. Detection mode: Multiple Reaction Monitoring (MRM). Curtain
57 gas pressure at 35.0 psi; spray voltage at –4500 V; nebulizer temperature at 550°C;
58 nebulizer gas pressure at 55 psi; auxiliary gas pressure at 60 psi.

59 1.1.3 Material analysis

60 Qualitative Analysis: One precursor ion and two product ions were selected
61 for monitoring the target compounds. Under the same experimental conditions, the
62 absolute value of the relative deviation between the retention time of the target
63 compound in the sample and that in the standard sample should be less than 2.5%;
64 and the relative abundance of the qualitative product ions (K_{sam}) of the target
65 compound in the sample compared with the relative abundance of the
66 corresponding qualitative product ions (K_{std}) in a standard solution of similar

67 concentration should not exceed the specified range, thus confirming the presence
68 of the corresponding target compound in the sample.

$$69 \quad K_{sam} = \frac{A_2}{A_1} \times 100\% \quad (1)$$

70 Where:

71 K_{sam} is the relative abundance of the qualitative product ions of the target
72 compound in the sample, %;

73 A_2 is the response value of the secondary mass spectrometry qualitative
74 product ions of the target compound in the sample;

75 A_1 is the response value of the secondary mass spectrometry quantitative
76 precursor ions of the target compound in the sample.

$$77 \quad K_{std} = \frac{A_{std2}}{A_{std1}} \times 100\% \quad (2)$$

78 Where:

79 K_{std} is the relative abundance ratio of the qualitative product ions of the target
80 compound in the standard sample, %;

81 A_{std2} is the response value of the secondary mass spectrometry qualitative
82 product ions of the target compound in the standard sample;

83 A_{std1} is the response value of the secondary mass spectrometry quantitative
84 precursor ions of the target compound in the standard sample.

K_{std} (%)	K_{sam} Tolerated Deviation (%)
$K_{std} > 50$	± 20
$20 < K_{std} \leq 50$	± 25
$10 < K_{std} \leq 20$	± 30
$K_{std} \leq 10$	± 50

85 The mass concentrations of 17 perfluoro compounds in the samples were
86 calculated using the following formula:

$$87 \quad \rho_i = \frac{x_i \times m_{is}}{V_w} \quad (3)$$

88 Where:

89 ρ_i is the mass concentration of the i th perfluoro compound in the sample;

90 x_i is the concentration ratio of the i th perfluoro compound to the corresponding
91 internal standard calculated from the calibration curve;

92 m_{is} is the added mass of the internal standard corresponding to the i th
93 perfluoro compound;

94 V_w is the sample volume.

95 1.2 Source Apportionment

96 The PMF model, which is widely applied as a receptor model (Paatero, 1997;
97 Paatero and Tapper, 1994), divides the sample data matrix into two (factor
98 contribution (G) and feature profile (F)) to quantitatively identify the source of
99 contaminants. The factor contributions and profiles were derived via the PMF model
100 by minimizing the objective function Q.

101 The two matrices (factor contributions (G) and factor profiles (F)), as described
102 in the following:

$$103 \quad X = G \times F + E \quad (4)$$

104 where X, the data matrix, is the $n \times m$ matrix of the m measured chemical species
105 in n samples; F is a $p \times m$ -matrix with rows that represent the emission profiles of p
106 factors; and G, an $n \times p$ -matrix with columns that represent the scores of p factors.
107 Matrix E is the residual matrix.

108 Factor contributions and profiles were derived by the PMF model by minimizing
109 the objective function Q, as described in the following:

$$110 \quad Q = \sum_{i=1}^n \sum_{j=1}^m \left[\frac{e_{ij}}{u_{ij}} \right]^2 \quad (5)$$

111 where e_{ij} is the residual of the j th chemical component in the i th sample, and u_{ij} is
112 the uncertainty of the j th chemical component in the i th sample.

113 According to the previous studies (Jiang et al., 2018), uncertainty is calculated as
114 follows (Equation 6):

115

$$116 \quad u_{ij} = \begin{cases} 0.2 * c_{ij} + MDL/3 & u_{ij} \leq MLD \\ 0.1 * c_{ij} + MDL/3 & u_{ij} > MLD \end{cases} \quad (6)$$

117 where u_{ij} is the uncertainty of the j_{th} chemical component in the i_{th} sample, c_{ij} is
118 the concentration of the j_{th} chemical component in the i_{th} sample. The missing data is
119 instead by species median, and the outliers are excluded from the PMF analysis. More
120 other details were described in the PMF 5.0 User Guide (Yu et al., 2009).

121 The chemical database used for the PMF consisted of PFAAs, PFBA, PFPeA,
122 PFHxA, PFHpA, PFOA, PFNA, PFDA, PFUnDA, PFDoDA, PFTTrDA, PFTeDA,
123 PFHxDA, PFOA, PFBS, PFHxS, PFOS, PFDS, giving a total of 22 species. In this
124 study, the overall number of samples and the number of variables complies with the
125 ratio of at least 3/1, as proposed by Belis et al (Belis et al., 2015).

126 All the included species were defined from weak to strong in the PMF based on
127 their signal-to-noise ratio (S/N). The PM species were categorized as “bad” when the
128 S/N ratio were below 0.2; “weak” when the S/N ratio were between 0.2 and 2; and
129 “strong” when the S/N ratio were higher than 2 (Esmaeilirad et al., 2020). The bad
130 species are excluded from the analysis while the uncertainty for the weak species is
131 tripled. PFAAs was defined as a “total variable” and was automatically categorized as
132 “weak”. All the included species were well reconstructed and were qualified as
133 “strong”.

134 The program was run several times to find the smallest value of Q_{expect} and to
135 reduce the observed value of residual error matrix E as much as possible in order to
136 ensure that the simulation results show a good correlation with the observations. The
137 stability of a PMF solution was estimated based on the bootstrap (BS), displacement
138 (DISP), and BS-DISP results (US EPA., 2014). After running the program several
139 times, the number of sources was set from two to six, and the results of four sources
140 were selected due to their adequate fit to the measurement data and their physical

141 meaning (more details can be found in Table S2). When the DISP analysis results
142 were 4 factors, no factor exchange occurred, indicating that the results were relatively
143 stable. Each factor mapping of the 4 factor results of BS analysis is greater than 80%,
144 indicating that the uncertainty of BS is acceptable and the number of factors is
145 reasonable. The PMF results were constrained with dQrobust of 0.59% and Fpeak =
146 0.0 produced the most physically reasonable source profiles.

147 1.3 Average Daily Inhalation (ADI) and Estimated Daily Intake (EDI)

148 Calculation

149 Median concentrations were utilized for data analysis in lieu of mean values, a
150 choice necessitated by the presence of extreme values (Huang et al., 2021).
151 Reference-based methods were employed to calculate the EDI and annual exposure
152 dosages (AEDs) for adults (Liu et al., 2017; Liu et al., 2023). The two calculations are
153 as follows:

$$154 \text{ ADI} = \frac{\rho \times \text{IR} \times \text{EF} \times \text{ED}}{\text{BW} \times \text{AT}} \quad (7)$$

$$155 \text{ EDI} = \rho \times \text{IR} \quad (8)$$

$$156 \text{ AED} = \text{EDI} \times \text{EF} \times \text{DR} \quad (9)$$

157 where ADI is average daily inhalation ($\text{pg} \cdot (\text{kg} \cdot \text{d})^{-1}$), ρ is the daily concentration
158 of each PFAAs ($\text{pg} \cdot \text{m}^{-3}$), IR is the adult inhalation rate ($15.73 \text{ m}^3 \cdot \text{day}^{-1}$), EF is the
159 annual exposure frequency ($350 \text{ days} \cdot \text{year}^{-1}$), ED is burst time (72 a), BW is adult
160 weight (65.0 kg), AT is average time ($72 \text{ a} \cdot 365 \text{ d} \cdot \text{a}^{-1}$), EDI is estimated daily intake
161 (pg), and DR is the detection rate of the compound.

162 **2. Tabulation**

163 Table. S1. PFAAs CIS and corresponding internal standard substance

Compound	CAS	Internal Standard	Mark recovery (%)	MDL (ng/L)	Retention time (min)
PFBA	375-22-4	¹³ C ₄ PFBA	97.49~112.02	0.3	2.7
PFPeA	2706-90-3	¹³ C ₄ PFBA	73.61~112.98	0.2	3.9
PFHxA	307-24-4	¹³ C ₄ PFHxA	94.84~115.89	0.2	5.1
PFHpA	375-85-9	¹³ C ₄ PFHxA	71.74~111.84	0.2	5.4
PFOA	335-67-1	¹³ C ₄ PFOA	91.04~117.75	0.3	6.1
PFNA	375-95-1	¹³ C ₄ PFNA	92.55~112.96	0.2	6.9
PFDA	335-76-2	¹³ C ₄ PFDA	96.81~115.60	0.2	7.5
PFUnDA	2058-94-8	¹³ C ₄ PFUnDA	96.81~115.24	0.2	7.8
PFDoDA	307-55-1	¹³ C ₂ PFDoDA	97.46~116.71	0.2	8.6
PFTTrDA	72629-94-8	¹³ C ₂ PFDoDA	96.88~110.99	0.3	9.2
PFTeDA	376-06-7	¹³ C ₂ PFDoDA	98.10~113.01	0.2	9.4
PFHxDA	67905-19-5	¹³ C ₂ PFDoDA	99.38~118.08	0.3	10.2
PFODA	16517-11-6	¹³ C ₂ PFDoDA	85.64~104.97	0.2	10.8
PFBS	375-73-5	¹⁸ O ₂ PFHxS	71.27~106.25	0.3	11.0
PFHxS	355-46-4	¹⁸ O ₂ PFHxS	89.91~102.78	0.3	11.8
PFOS	1763-23-1	¹³ C ₄ PFOS	96.42~111.07	0.3	13.2
PFDS	335-77-3	¹³ C ₄ PFOS	97.56~109.07	0.2	14.4
¹³ C ₄ PFBA					2.7
¹³ C ₄ PFHxA					5.1
¹³ C ₄ PFOA					6.9
¹³ C ₄ PFNA					7.5
¹³ C ₄ PFDA					7.8
¹³ C ₄ PFUnDA					8.6
¹³ C ₂ PFDoDA					9.2
¹⁸ O ₂ PFHxS					9.4
¹³ C ₄ PFOS					10.2

Table. S2. Summary of PMF and error estimation diagnostics from two to six factors.

Factor number	PMF				
	2	3	4	5	6
Q_{robust}	15289	11948	11021	9936	7941
Q_{true}	21987	16238	13123	11071	9375
Q_{expected}	1480	1301	1219	1189	1048
$Q_{\text{true}}/Q_{\text{expected}}$	14.85608108	12.48117	10.76538	9.311186	8.945611
$Q_{\text{robust}}/Q_{\text{expected}}$	10.33040541	9.183705	9.041017	8.356602	7.57729
DISP%dQ	0	0	0	0	0
DISP swaps	0	0	0	0	0
Factor with BS mapping < 80%	All factor > 80%	factor 3, 47%	All factor > 80%	factor 3, 65%, factor 4, 33%,	factor 1, 41%, factor 5, 63%, factor 6, 71%

Table. S3. Atmospheric PM_{2.5} sample information table

Sampling time	Samples quantity	Sampling volume (m ³)	Membrane diameter (mm)	Sample type
Spring	15	3.25	90	Urban atmospheric PM _{2.5} sample
Summer	15	3.25	90	
Autumn	15	3.25	90	
Winter	15	3.25	90	

3. Figure

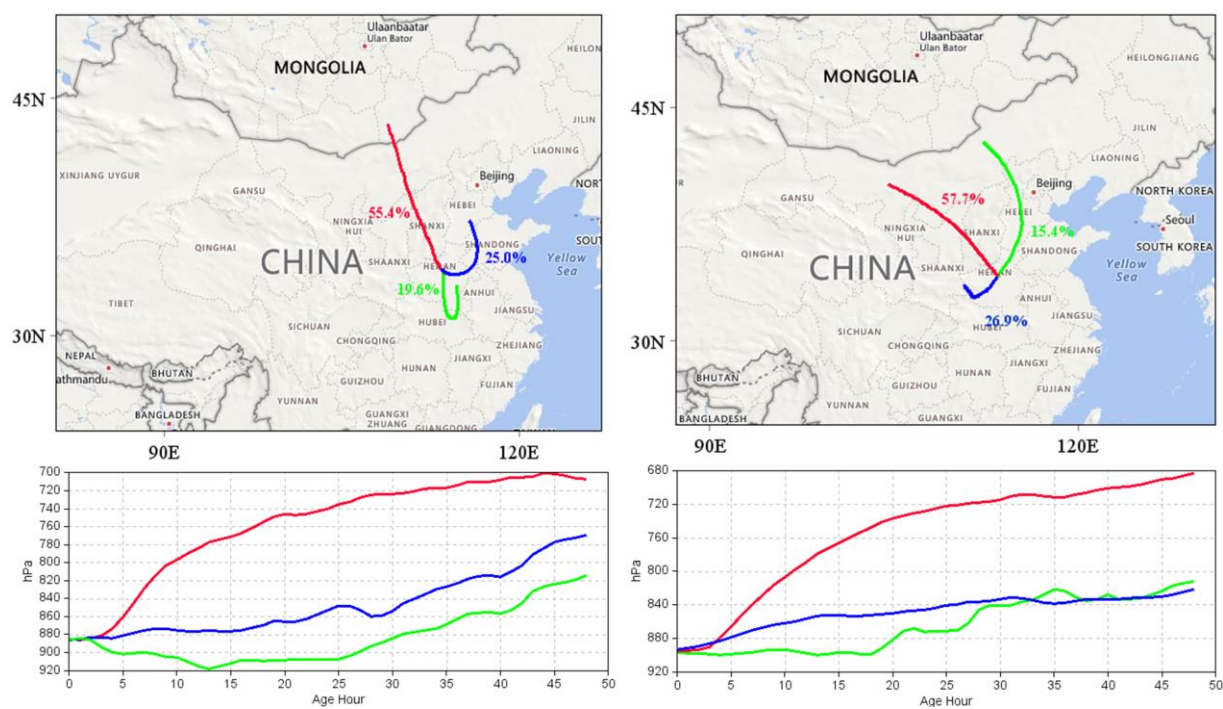


Fig. S1. Cluster analysis map of backward trajectories in Zhengzhou City (left and right are summer and autumn respectively, created by MeteInfoMap 3.5.11 (Wang, 2014; Wang, 2019)). © Microsoft. The software is open.

References

- Belis, C.A., Karagulian, F., Amato, F., Almeida, M., Artaxo, P., Beddows, D.C.S., et al., 2015. A new methodology to assess the performance and uncertainty of source apportionment models II: The results of two European intercomparison exercises. *Atmos. Environ.* 123, 240-250. <http://dx.doi.org/10.1016/j.atmosenv.2015.10.068>
- Esmailirad, S., Lai, A., Abbaszade, G., Schnelle-Kreis, J., Zimmermann, R., Uzu, G., et al., 2020. Source apportionment of fine particulate matter in a Middle Eastern Metropolis, Tehran-Iran, using PMF with organic and inorganic markers. *Sci. Total. Environ.* 705. <http://dx.doi.org/10.1016/j.scitotenv.2019.135330>
- Huang, W., Shi, Y., Huang, J., Deng, C., Tang, S., Liu, X., et al., 2021. Occurrence of Substituted ρ -Phenylenediamine Antioxidants in Dusts. *Environ. Sci. Technol. Lett.* 8, 381-385. <http://dx.doi.org/10.1021/acs.estlett.1c00148>
- Jiang, N., Yin, S., Guo, Y., Li, J., Kang, P., Zhang, R., et al., 2018. Characteristics of mass concentration, chemical composition, source apportionment of PM_{2.5} and PM₁₀ and health risk assessment in the emerging megacity in China. *Atmos. Pollut. Res.* 9, 309-321. <http://dx.doi.org/10.1016/j.apr.2017.07.005>
- Liu, J., Wang, Y., Le, P.-H., Shou, Y.-P., Li, T., Yang, M.-M., et al., 2017. Polycyclic Aromatic Hydrocarbons (PAHs) at High Mountain Site in North China: Concentration, Source and Health Risk Assessment. *Aerosol Air Qual. Res.* 17, 2867-2877. <http://dx.doi.org/10.4209/aaqr.2017.08.0288>
- Liu, L.-S., Guo, Y.-T., Wu, Q.-Z., Zeeshan, M., Qin, S.-J., Zeng, H.-X., et al., 2023. Per- and polyfluoroalkyl substances in ambient fine particulate matter in the Pearl River Delta, China: Levels, distribution and health implications. *Environ. Pollut.* 334. <http://dx.doi.org/10.1016/j.envpol.2023.122138>
- Paatero, P., 1997. Least squares formulation of robust non-negative factor analysis. *Chemometrics Intell. Lab. Syst.* 37, 23-35. [http://dx.doi.org/10.1016/s0169-7439\(96\)00044-5](http://dx.doi.org/10.1016/s0169-7439(96)00044-5)
- Paatero, P., Tapper, U., 1994. POSITIVE MATRIX FACTORIZATION - A NONNEGATIVE FACTOR MODEL WITH OPTIMAL UTILIZATION OF ERROR-ESTIMATES OF DATA VALUES. *Environmetrics.* 5, 111-126. <http://dx.doi.org/10.1002/env.3170050203>
- US EPA. Positive matrix factorization (PMF) 5.0 fundamentals and user guide [EB]. Office of Research and Development, Washington, DC, 2014.
- Wang, Y. Q., 2014. Meteolnfo: GIS software for meteorological data visualization and analysis. *Meteorol. Appl.* 21, 360-368. <https://doi.org/10.1002/met.1345>
- Wang, Y. Q., 2019. An Open Source Software Suite for Multi-Dimensional Meteorological Data Computation and Visualisation. *Journal of Open Research Software.* 7, 21. <https://doi.org/10.5334/jors.267>
- Yu, Y., Galle, B., Panday, A., Hodson, E., Prinn, R., Wang, S., 2009. Observations of high rates of NO₂-HONO conversion in the nocturnal atmospheric boundary layer in Kathmandu, Nepal. *Atmos. Chem. Phys.* 9, 6401-6415. <http://dx.doi.org/10.5194/acp-9-6401-2009>